Proceedings of the Pakistan Academy of Sciences: A Physical and Computational Sciences 59(4): 25-35 (2022)
Copyright © Pakistan Academy of Sciences
ISSN (Print): 2518-4245; ISSN (Online): 2518-4253
https://doi.org/10.53560/PPASA(59-4)783

Pakistan Academy of Sciences

Research Article

Modeling and Intelligent Controller Design for Reactor Regulating System of Advanced CANDU Reactor (ACR-700) in LabVIEW

Arshad Habib Malik[1*], Feroza Arshad[2], and Aftab Ahmad Memon[3]

[1]Department of Basic Training, Chashma Centre of Nuclear Training, Pakistan Atomic Energy Commission, Chashma, Pakistan
[2]Department of Information System, Karachi Nuclear Power Generating Station, Pakistan Atomic Energy Commission, Karachi, Pakistan
[3]Department of Telecommunication Engineering, Mehran University of Engineering and Technology, Jamshoro, Pakistan

Abstract: In this research work, an Advanced CANDU Reactor of 700 MWe rating (ACR-700) is attempted for Reactor Regulating System (RRS) modeling and intelligent controller design. ACR-700 is a state-of-the-art advanced generation-III reactor. The reactor regulating system is modeled with special emphasis on internal and external reactivity devices. ACR-700 is designed with Liquid Zone Control (LZC) Model, Adjuster Banks Model, Absorber Banks Model and Shutdown Banks Model. The RRS model is a highly sophisticated model developed based on the principle of spatial nuclear reactor dynamics. The RRS model is a multivariable model. The spatial reactor dynamics is modeled based on five internal feedbacks and three feedbacks. The original controller design of RRS is comprised of a PID control algorithm. The control design is reattempted with an advanced intelligent algorithm in which the ANFIS controller is used as a modern control design tool. The new ANFIS controller is basically a multivariable controller. All the modeling of RRS is implemented in Visual Basic (VB) Software while the controller is configured in LabVIEW. A special toolkit is designed for the interfacing of Visual Basic and LabVIEW known as VBLAB. The optimization of intelligent controller parameters is carried out by Genetic Algorithm (GA). The GA-optimized intelligent controller is configured with the VB RRS model. All the variable trends are visualized in the VB environment. The proposed closed-loop ACR-700 RRS control system is tested for small perturbation Analysis and power ramp-down transient and found with excellent behavior well within the design limits. The performance of the suggested ACR-700 RRS controller is compared with the existing conventional controller. The performance of the suggested control scheme is marked with reduced oscillations and faster as compared to the existing control scheme.

Keywords: Spatial Reactor Dynamics, Intelligent Controller, GA Optimization, ACR-700, LabVIEW.

1. INTRODUCTION

A third-generation advanced CANDU reactor of 700 MWe rating is considered for modeling, control design and simulation purposes in the present research. The PWR reactor dynamics based on the first principle is addressed by Johnson *et al*. [1]. Coupled transient neutronics calculations are performed by Lam *et al*. [2] for the molten fast reactor. A PWR design tool is developed by Mollah *et al*. [3] for safety and transient analysis. The reactor kinetics simulator is designed by Hakim *et al*. [4] for research reactor in LabVIEW. A deep learning based multi-model oriented PWR dynamics is modeled by Malik *et al*. [5] in LabVIEW. A PWR controller is designed by Mousakazemi *et al*. [6] for two-point reactor kinetics model and optimized using PSO. The PWR reactor regulating system is improved by Shim *et al*. [7] optimized by genetic algorithm. The CANDU reactor regulating system is analyzed by Cho *et al*. [8] in detail for safety analysis modeled in CATHENA computer code. A safety simulator for CANDU reactor using first principle point reactor kinetics of ACR-700 is modeled by

Received: August 2022; Accepted: December 2022
*Corresponding author: Arshad Habib Malik <engr.dr.arshad.habib.malik@gmail.com>

Boroni *et al*. [9]. A global power-based reactor regulating system of 540 MWe PHWR is addressed by Subudhi *et al*. [10]. A reactor power regulator is modeled by Volodin *et al*. [11] for CANDU-6 based on parametric settings. A modeling and spatial power controller is performed by Tiwari *et al*. [12] for 540 MWe PHWR. Research is extended by Banerjee *et al*. [13] for 700 MWe PHWR with voiding effect. An attempt is made by Darling *et al*. [14] for intelligent modeling of sodium fast reactor-based nuclear power plant for safety accident management. An Adaptive Neuro-Fuzzy Inference System (ANFIS) based intelligent controller is designed by Malik *et al*. [15] for ACP1000 nuclear power plant in LabVIEW. A detailed safety study is carried out by Shidik *et al*. [16] for ACR-700 using ACR-700 simulator in LabVIEW.

In this research work, a novel spatial reactor dynamics model of reactor regulating system of advanced CANDU reactor of 700 MWe is developed. For RRS model of ACR-700, a new discrete PID controller algorithm is developed and modern ANFIS based intelligent controller is designed and performance is evaluated. The configuration of RRS model and controller synthesis is a novel special hybrid integration of Visual Basic Software and LabVIEW Software resulting in novel development of VBLAB Toolkit. The performance of proposed intelligent controller with new gains is much smooth, oscillation free, faster and robust in reference tracking mode.

2. MATERIALS AND METHODS

2.1 ACR-700 Reactor Regulating System

ACR-700 reactor regulating system is a highly advanced and sophisticated system meant for fine and coarse power control of advanced CANDU nuclear power plant of 700 MWe. It consists of reactivity control devices. The block diagram of liquid zone control system is shown in Figure 1. Liquid zone control system consists of delay tank, liquid zone pump, liquid zone inlet control valve, liquid zone outlet isolation valve, liquid zone and PID controller.

The reactivity control in liquid zone control system is appended by incorporating reactor and rate limiter as shown in Figure 2.

The configuration of liquid zones in ACR-700 is shown in Figure 3. However, the physical visualization of liquid zones is shown in Figure 4. Practically, seven liquid zone compartments are installed in upper face while other seven are installed in lower face. The water in each liquid zone compartment is light water while moderator in Calandria is heavy water. The neutronics characteristics of both light and heavy water are entirely different. The absorption and scattering cross-sections of light water is more as compared to heavy water.

The block of complete reactor regulating system of ACR700 is shown in Figure 5.

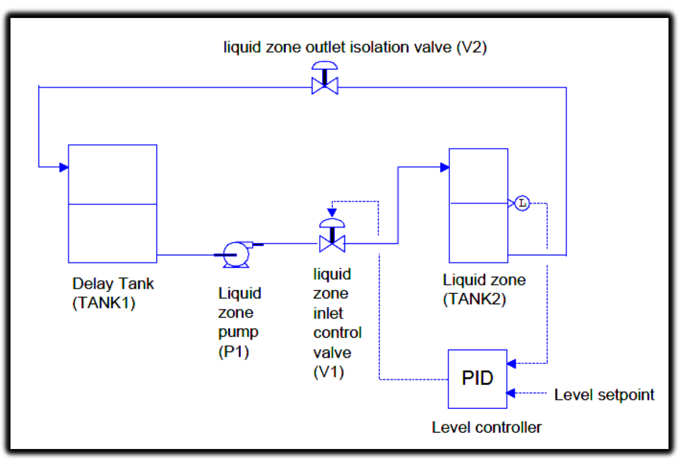

Fig. 1. Block Diagram of Liquid Zone Control System in ACR700

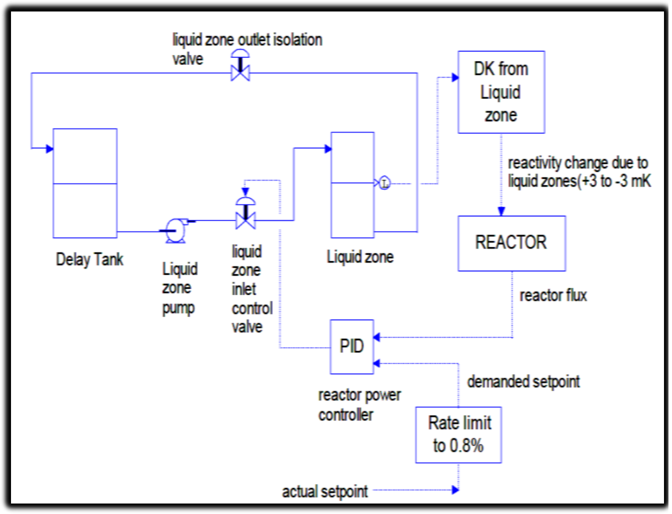

Fig. 2. Block Diagram of Reactivity Control in Liquid Zone Control System in ACR700

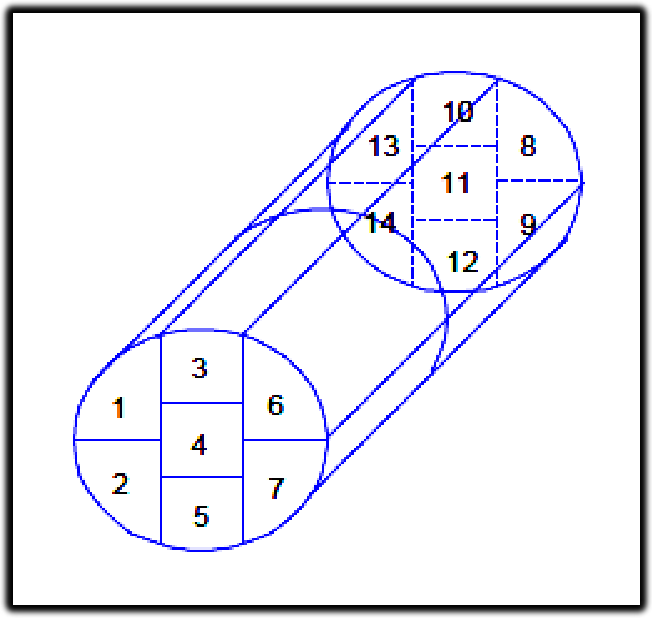

Fig. 3. Configuration of Liquid Zones in ACR700

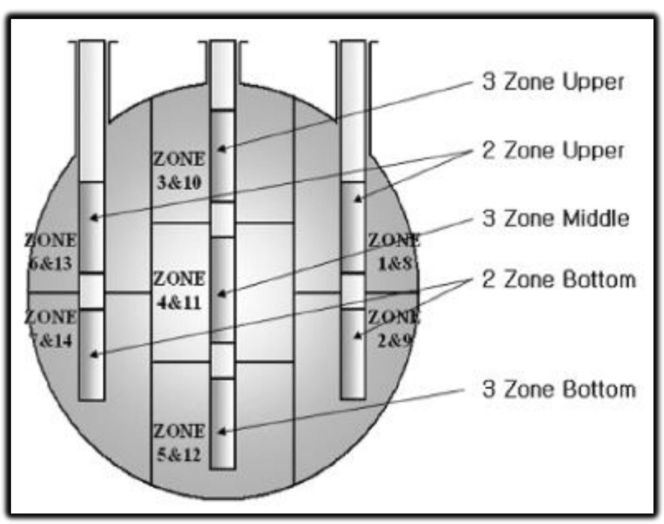

Fig. 4. Physical Visualization of Liquid Zones in ACR700

The reactor regulating system consists of fourteen liquid zones and corresponding fourteen liquid zone controllers. The water level in each zone is controlled by control valve governed by liquid zone controller. In each zone, in addition to liquid zone, there is an effect of adjuster rods, absorber rods, shut down rods and fuel burn-up. The reactor zone flux and water level in the zone is fed to liquid zone controller. Average zone level, average zone flux and power error signals are also fed to each liquid zone controller.

2.2 ACR-700 Reactor Regulating System Modeling

The reactor regulating system is modeled using i-th nodes, six fission fragments groups (j-th precursor groups) and fourteen liquid zones (k-th zones) based on spatial point kinetic model as:

$$l_i \frac{dn_i(t)}{dt} = (1-\beta)\sum_{k=1}^{14}\alpha_{ik}n_k - n_i(t) + \sum_{k=1}^{14}\alpha_{ik}\sum_{i=1}^{6}\lambda_j C_{jk} \quad (1)$$

$$\frac{dC_{jk}(t)}{dt} = \beta_j n_k(t) - \lambda_j C_{jk}(t) \quad (2)$$

Where the symbols having their usual meanings.

On re-grouping the coupling coefficients and using the definition of reactivity, equations (1) is redefined as:

$$\frac{dn_i(t)}{dt} = \frac{(\Delta K_i - \beta)}{\Lambda_i} n_i(t) + \sum_{j=1}^{6}\frac{\lambda_j}{l_i} C_{ji}(t)$$

$$+ \frac{(1-\beta)}{l_i}\sum_{k=1,k\neq i}^{14}\alpha_{ik}n_i(t) + \frac{1}{l_i}\sum_{k=1,k\neq i}^{14}\alpha_{ik}\sum_{j=1}^{6}\lambda_j C_{jk}(t) \quad (3)$$

The overall internal reactivity change is given as:

$$\Delta K_{in}(t) = \Delta K_P(t) + \Delta K_V(t) + \Delta K_{Xe}(t) + \Delta K_{FUEL}(t) \quad (4)$$

The overall external reactivity change is given as:

$$\Delta K_{ex}(t) = \Delta K_{LZC}(t) + \Delta K_{ADC}(t) + \Delta K_{ABC}(t) \quad (5)$$

The overall reactivity change is given as:

$$\Delta K_i(t) = \Delta K_{in}(t) + \Delta K_{ex}(t) + \Delta K_{SDS}(t) + \Delta K_{\alpha_{ik}Z}(t) \quad (6)$$

Various parameters/symbols and variables used in the above section are defined as following:

n(t) = Reactor Power
C(t) = Precursor Concentration
β = Delayed Neutron Fraction
α = Coupling Coefficient
t = Neutron Life Time
ΔK = Change in Reactivity
ΔKin = Change in Internal Reactivity
ΔKex = Change in External Reactivity
ΔKP = Change in Reactivity due to Power
ΔKFUEL = Change in Reactivity due to Fuel
ΔKV = Change in Reactivity due to Voiding
ΔKP = Change in Reactivity due to Power
ΔKXe = Change in Reactivity due to Xenon
ΔKP = Change in Reactivity due to Power
ΔKLZC = Change in Reactivity due to Liquid Zone Control
ΔKADC = Change in Reactivity due to Adjuster
ΔKABC = Change in Reactivity due to Absorber
ΔKSDS = Change in Reactivity due to Shut Down System
H(k) = Liquid Zone Level
H(k-1) = Previous Liquid Zone Level
G = Gain

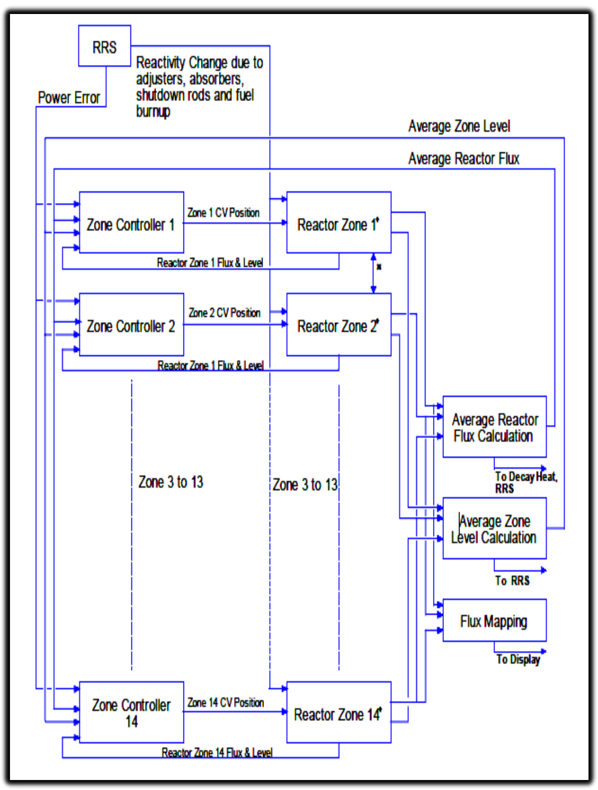

Fig. 5. Block Diagram of Reactor Regulating System (RRS) of ACR700

ep (k) = Power Error
K = Controller
μ = Membership Function

2.3 ACR-700 RRS Controller Framework

ACR-700 RRS controller is basically multivariable controller as shown in Figure 6.

Fig. 6 clearly shows that there are multiple set-points, multiple controlled variables and hence multiple manipulated variables.

The overall control framework of ACR-700 is shown in Figure 7. The primary coolant pressure and primary coolant flow are the disturbance signals. Figure 7 is the representation of Fig. 6 with actual details of inputs, outputs and disturbance variables used in ACR-700.

2.4 ACR-700 RRS Controller Modeling

The power error signal is computed as [6]:

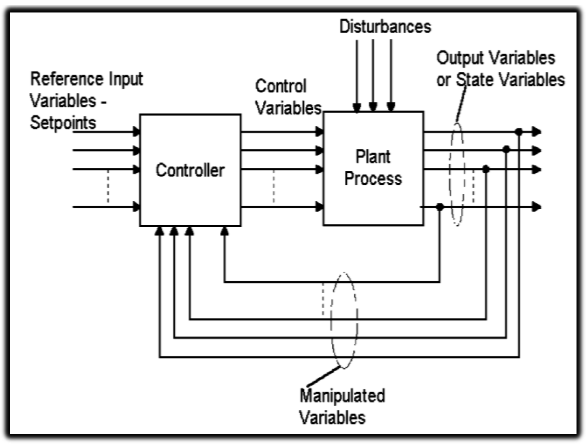

Fig. 6. Structure of Multivariable RRS Closed Loop System of ACR700

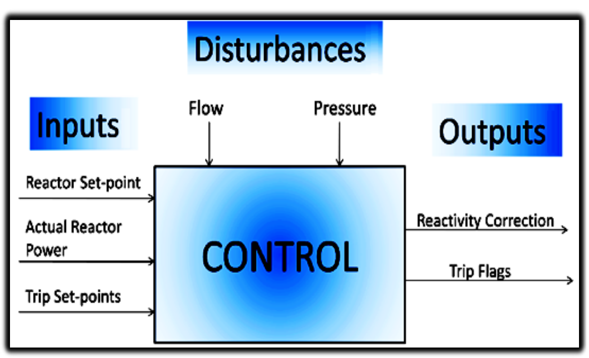

Fig. 7. Overall Control Framework of RRS in ACR700

$$e_P(k) = K_P \frac{[n_r(k) - n_D(k)]}{n_r(k)} + K_D\left[\frac{[n_r(k) - n_r(k-1)]}{[n_r(k)\Delta t]} - \frac{[n_r(k) - n_D(k)]}{\Delta t}\right] \quad (7)$$

The power tilt in the i-th cell of reactor core is given as:

$$P_{Ti} = K_T[n_{r_i}(k) - n_r(k)] \quad (8)$$

The bulk power control is accomplished by 8 representative zones using speed algorithm as:

$$\frac{[LZC - H(k) - LZC - H(k-1)]_k}{\Delta t} = G_1 e_P(k) + G_2 P_T + K_H[H_k(k) - H_{AV8Z}(k)] \quad (9)$$

The spatial power control is accomplished by 10 representative zones using speed algorithm as:

$$\frac{[LZC - H(k) - LZC - H(k-1)]_k}{\Delta t} = G_3 e_P(k) + G_4[H_{AV8Z}(k) - 0.5] + G_5[H_{AV10Z}(k) - H_k(k)] \quad (10)$$

Where the parameters/symbols have their usual meanings.

2.5 Optimization of ACR-700 RRS Existing Controller

The optimization of existing ACR-700 RRS controller is accomplished in LabVIEW as shown in Figure 8.

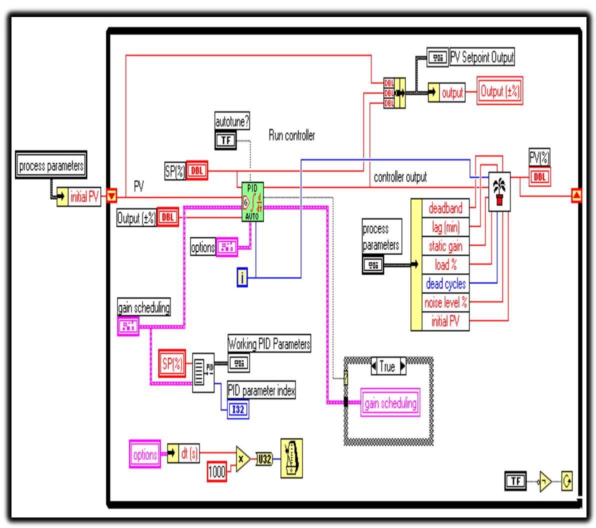

Fig. 8. Block Diagram Design for ACR700 PID Controller Design in LabVIEW

2.6 Configuration of New ACR-700 RRS Control System

The ACR-700 RRS model is configured in VB while ACR-700 RRS controller is configured in LabVIEW. The integration scheme of LabVIEW and Visual Basic is shown in Figure 9.

Fig. 9 shows the logical flow of model and controller variables transfer scheme. This scheme is basically the client and server configuration. The server configuration is in LabVIEW while the client configuration is in Visual Basic.

The configuration of new ACR-700 RRS control system is shown in Figure 10.

2.7 Intelligent ACR-700 RRS Controller Modeling

The intelligent ACR-700 RRS controller output with MISO configuration in discrete domain is given as [15]:

$$K = \frac{\sum_{l=1}^{L}\left(\frac{(\mu A_l(x)\mu B_l(y))(p_l x + q_l y + r_l)}{\sum_{l=1}^{L}(\mu A_l(x)\mu B_l(y))}\right)}{\sum_{l=1}^{L}(\mu A_l(x)\mu B_l(y))} \quad (11)$$

Where the parameters/symbols have their usual meanings.

2.7.1 *Intelligent Controller Design for ACR-700 RRS Controller in LabVIEW*

The ANFIS controller is configured in LabVIEW. The front panel design is shown in Figure 11. The block diagram of intelligent ACR-700 RRS controller is shown in Figure 12.

2.7.2 *Genetic Algorithm for Optimization of Intelligent ACR-700 RRS Controller*

A block diagram is designed for the process of GA initialization and optimization as shown in Figure 13. The block diagram design for the fitness function is shown in Figure 14.

3. RESULTS AND DISCUSSION

The modeling work is carried out in VB, control design, optimization and simulations work is carried out in LabVIEW.

3.1 Simulation of Proposed Closed Loop ACR-700 RRS Control System in Hybrid Framework

The detailed analysis of proposed closed loop ACR-700 RRS control system in hybrid framework is performed by taking into account the three distinct scenarios.

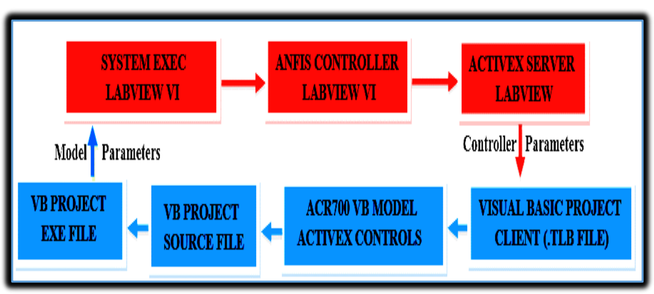

Fig. 9. Integration of LabVIEW and Visual Basic

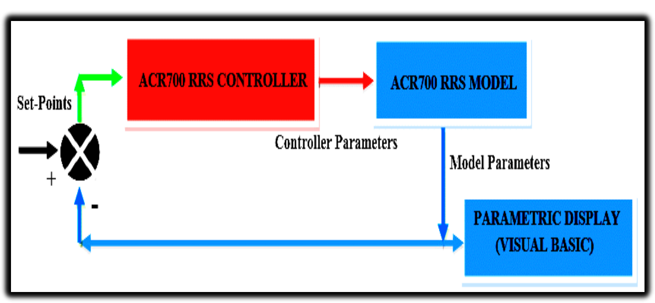

Fig. 10. Configuration of ACR700 RRS Controller and ACR700 RRS Model

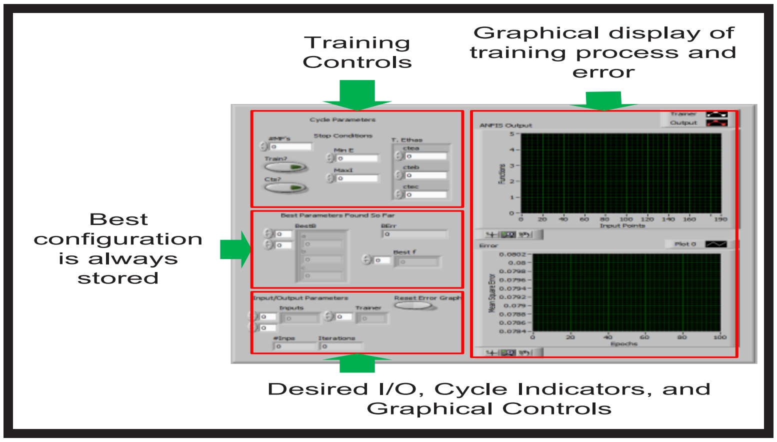

Fig. 11. Front Panel Design of ACR700 ANFIS RRS Controller in LabVIEW

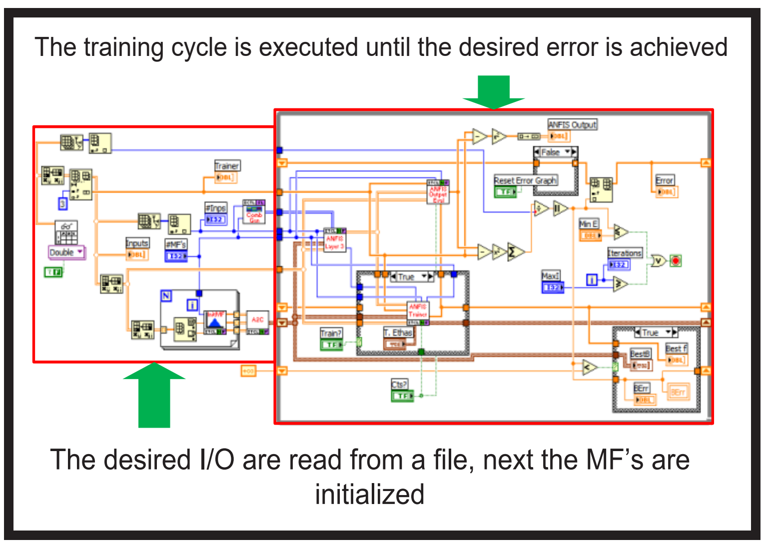

Fig. 12. Block Diagram Design of ACR700 ANFIS RRS Controller in LabVIEW

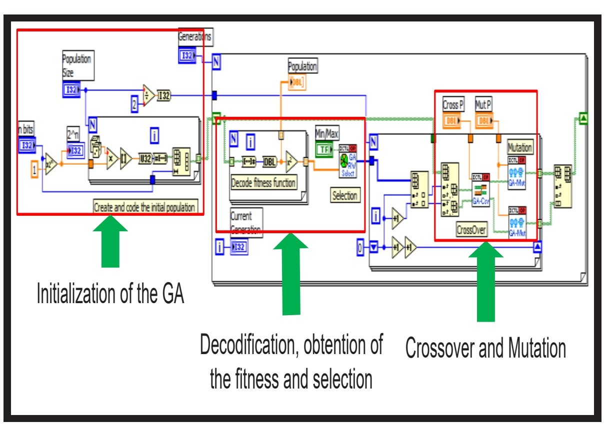

Fig. 13. Block Diagram Design of GA Optimization of ACR700 ANFIS RRS Controller in LabVIEW

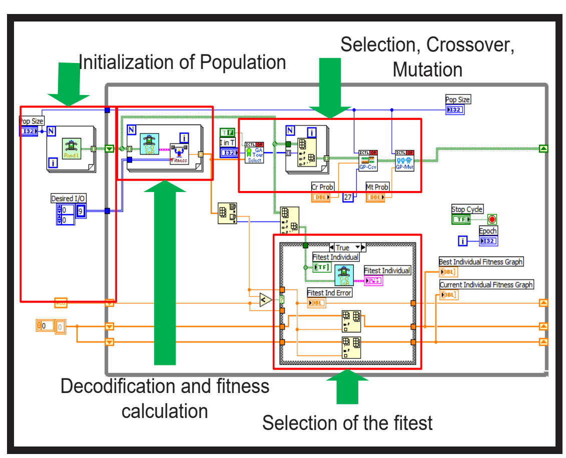

Fig. 14. Block Diagram Design for Fitness Function of GA Optimization for ACR700 ANFIS RRS Controller in LabVIEW

GA parameters are optimized based on RMSE value which is a function of PID controller output and ANFIS controller using premise parameters, consequent parameters and rules defined for the ACR-700 RRS. In this research work many attempts have been made and finally population size is chosen as 190, cross-over rate is chosen as 0.7 and mutation rate is chosen as 0.02.

In one scenario, the demand power is predicted against the set-point change as shown in Figure 15.

The power error is computed and hence the prediction of reactivity model is assessed as shown in Figure 16.

In this transient, set-point is changed in power step down fashion and hence the demanded power try to follow the set-point change based dynamics of liquid zone control system.

In second scenario, small perturbation analysis is performed, in which the reactor power is varied from 100% with ± 0. 2% i.e. the operating is 100% while deviation is allowed in steady state with maximum value of ± 0. 2% as shown in Figure 17.

The respond to this power maneuvering, the power error and compensated reactivity is computed as shown in Figure 18.

The total reactivity change of liquid zone control system against this power transient in compensation with all internal and external reactivity changes mentioned in section 2.2 is shown in Figure 19.

Now, the third scenario is selected in which the reactor power is ramp down from 100% to 98% as shown in Figure 20. Based on this power change, power error and reactivity are computed as shown in Figure 21. The power error is decreased and later on stabilized at the end of transient. Similarly, the compensated reactivity is increased as fuel burn-up is reduced and later on stabilized.

The total reactivity change due to liquid zone control is shown in Figure 22. This reactivity of liquid zone control is observed with increasing reactivity trend in compensation with all internal and external reactivity changes mentioned in section 2.2.

3.2 Performance Analysis of Proposed Closed ACR-700 RRS Control System

Now, special trending facility is developed in which performance of suggested closed loop ACR-700 RRS control system is compared with existing closed loop ACR-700 RRS control system.

Now, a low power transient is designed in which reactor power is varied from 25% to 30% through a power ramp-up transient as shown in Figure 23. This transient is designed because in ACR-700 dynamic transient at low power is the most challenging one due to highest system oscillations and fluctuations keeping in view that nuclear power plant control at low power is the most difficult scenario.

The existing control system takes oscillation at steady state while the suggested control system is found with remarkable performance and excellently tracking the set-point change.

Now the effective power error change against this transient is shown in Figure 24.

The average zone control compartment water level change is shown in Figure 25.

The zone control compartment water level error change is shown in Figure 26.

Hence, the performance of proposed closed loop ACR-700 RRS control system is proved fast, oscillation free and robust in performance in steady state, small perturbation, high power ramp-down transient and low power ramp-up transient. Therefore, the proposed control is proved an excellent practical possibility for advanced CANDU reactor such as ACR-700 nuclear power plant and future ACR-1000 nuclear power plant.

4. CONCLUSION

The reactor regulating system modeling and control of ACR-700 has been addressed in this research work. A spatial point reactor kinetics model with xenon dynamics, power dynamics, voiding dynamics, safety shut down systems dynamics, fuel burn-up dynamics, liquid control compartment dynamics, adjuster banks dynamics and absorber banks dynamics is developed in visual basic environment.

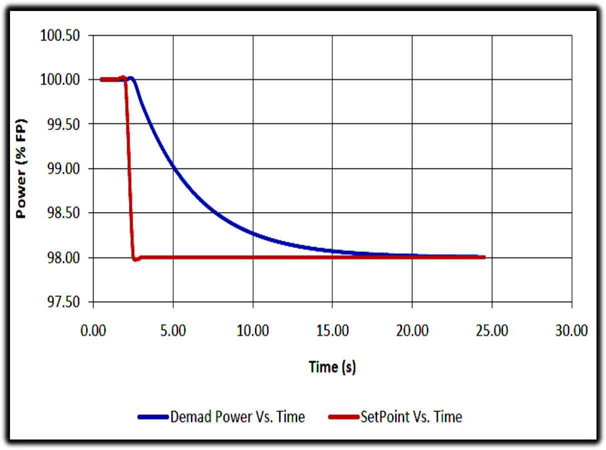

Fig. 15. Prediction of Demanded Power Model of ACR700 RRS

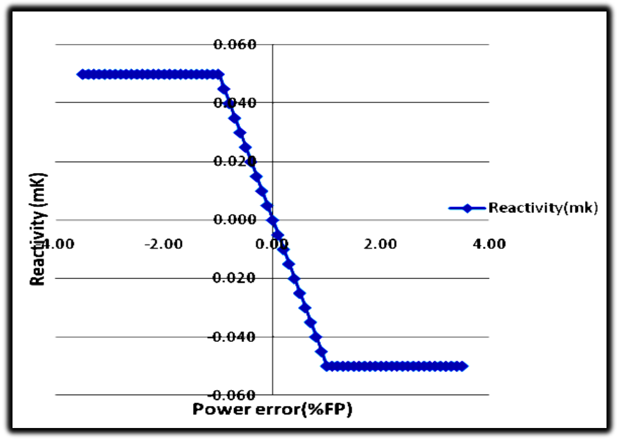

Fig. 16. Prediction of Power Error Dependent Reactivity Model of ACR700 RRS

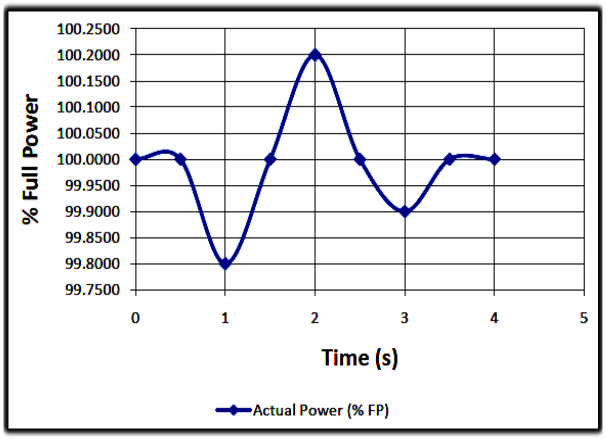

Fig. 17. Small Power Perturbation Maneuvering Transient in RRS of ACR700 RRS

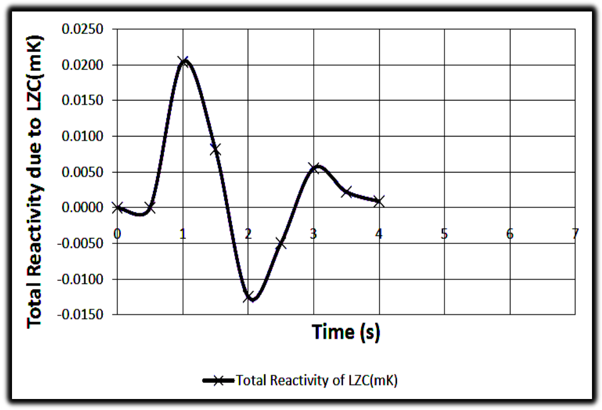

Fig. 18. Prediction of Power Error and Reactivity under Small Power Perturbation Maneuvering Transient of ACR700 RRS

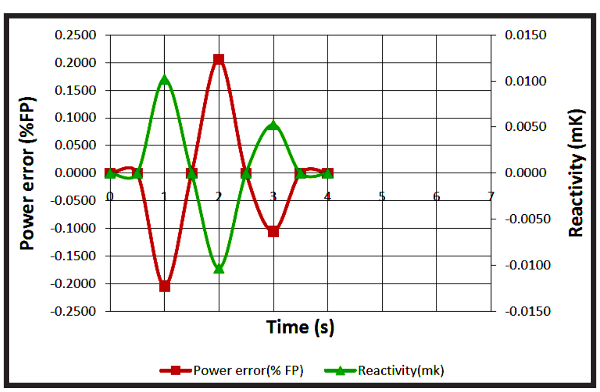

Fig. 19. Prediction of Total Reactivity of Liquid Zone Control System under Small Power Perturbation Maneuvering Transient of ACR700 RRS

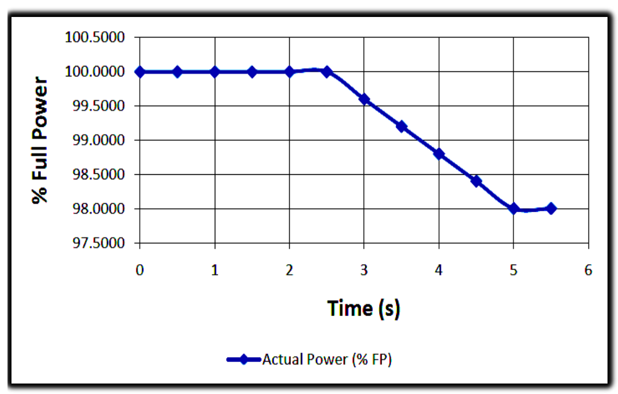

Fig. 20. Reactor Power Ramp-down Transient ACR700 RRS

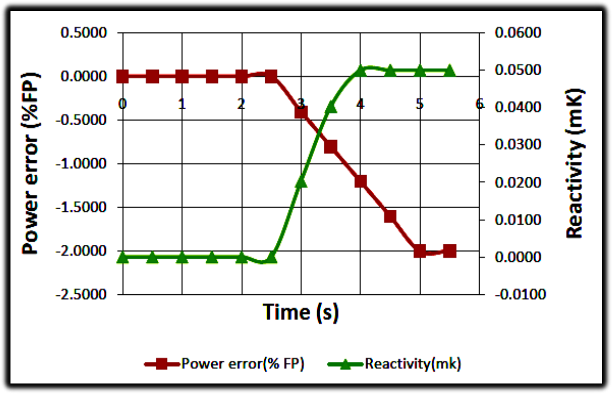

Fig. 21. Prediction of Power Error and Reactivity in Power Ramp-down Transient of ACR700 RRS

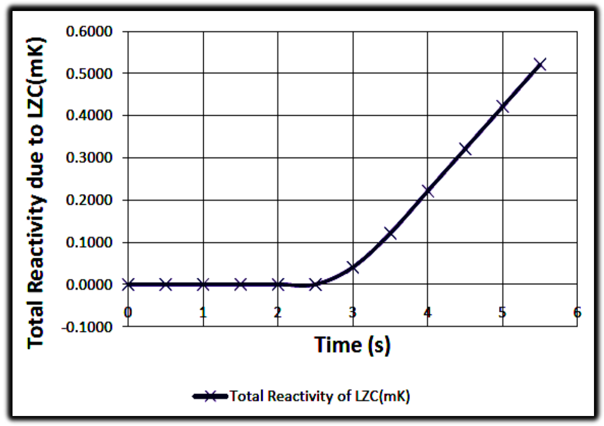

Fig. 22. Prediction of Total Reactivity of Liquid Zone Control System in Power Ramp-down Transient of ACR700 RRS

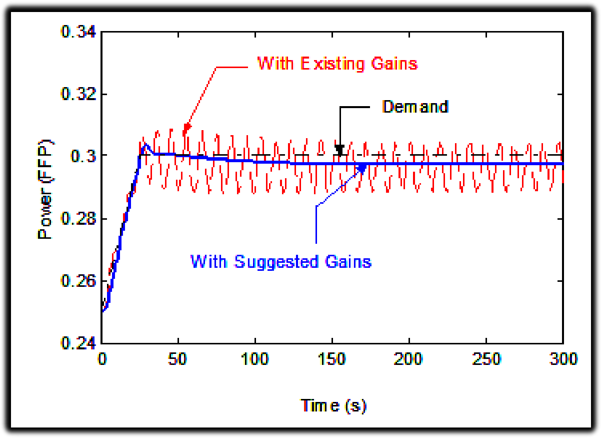

Fig. 23. Performance Comparison of Reactor Power under Low Power Transient for ACR700 RRS

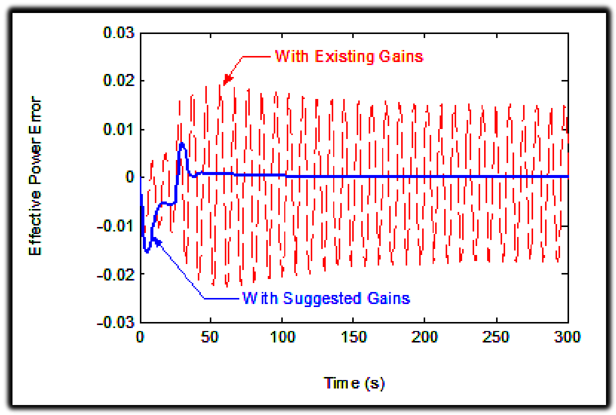

Fig. 24. Performance Comparison of Effective Reactor Power Error under Low Power Transient for ACR700 RRS

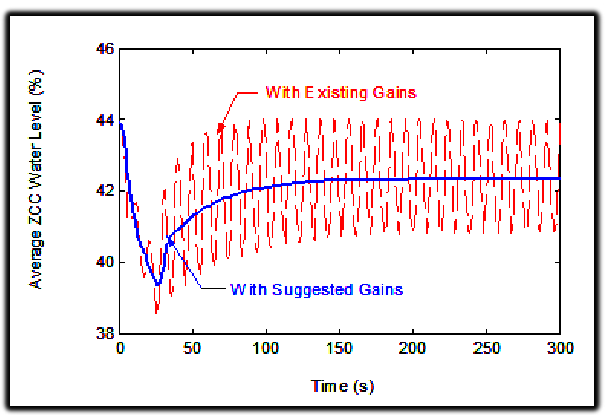

Fig. 25. Performance Comparison of Average Zone Control Compartment Water Level under Low Power Transient for ACR700 RRS

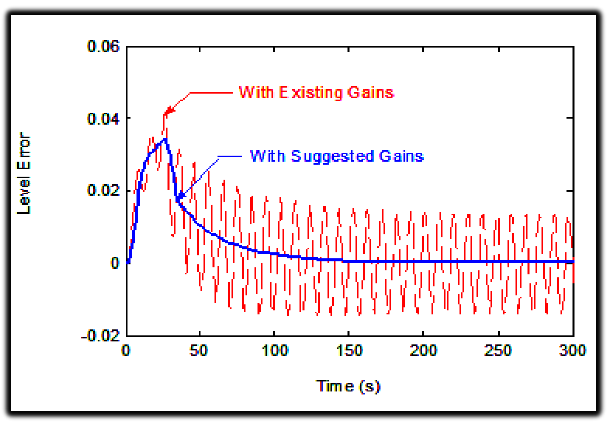

Fig. 26. Performance Comparison of Zone Control Compartment Water Level Error under Low Power Transient for ACR700 RRS

One PID controller as existing controller while other as ANFIS controller are configured with RRS model. Parameters or gains of the controllers are optimized in LabVIEW environment. A hybrid framework is designed and developed integrating VB and LabVIEW. As a result of this research work a sophisticated toolkit is developed called VBLAB. The performance of the suggested new ACR-700 RRS controller is compared existing controller and found faster, robust and within the designed control bands.

5. ACKNOWLEDGEMENT

The support of the Pakistan Atomic Energy Commission, Chashma Centre of Nuclear Training and Information Support Division of KNPGS is gratefully acknowledged.

6. CONFLICT OF INTEREST

The authors declare no conflict of interest.

7. REFERENCES

1. M. Johnson, S. Lucas, and P. Tsvetkov. Modeling of reactor kinetics and dynamics. *Idaho National Laboratory, Report Idaho Falls, Idaho 83415, U.S. Department of Energy, Canada* (2010).
2. W.K. Lam. Advanced pressurized water reactor simulator. *IAEA Workshop on NPP Simulators for Education, Bucharest, Romani*a (2006).
3. A.S. Mollah. Education tool for simulation of safety and transient analysis of a pressurized water reactor. *International Journal of Integrated Sciences & Technology* 03: 01-10 (2018).
4. S.U.E. Hakim, A. Abimanyu, and Sutanto. Simulator design of Kartini reactor based on LabVIEW. *Journal forum Nukir* 12: 29-41 (2018).
5. A.H. Malik, A. A. Memon, and F. Arshad. Advanced multi-modeling of PWR dynamics and deep learning based computational tool in SIMULINK and LabVIEW. *Proceedings of Pakistan Academy of Sciences-A: Physical and Computational Sciences* 59: 71-81 (2022).
6. S.M.H. Mousakazemi. Control of a pressurized light-water nuclear reactor two-point kinetics model with performance index-oriented PSO. *Nuclear Engineering and Technology* 53: 2556-2563 (2021).
7. H.S. Shim, and J.C. Jung. Improved RRS logical architecture using genetic algorithm. *Nuclear Engineering and Technology* 49: 1696-1710 (2017).
8. C.H. Cho, J.H. Choi, J.Y. Hoi, and S.Y. Lee. CANDU NPP reactor regulating system modeling using CATHENA. *Annulus of Nuclear Energy* 23: 909-918 (1996).
9. G. Boroni, and A. Clausse. Ladwig: A training simulator of the safety operation of a CANDU. *Science and Technology of Nuclear Installations*: 1-8 (2011).
10. C.S. Subudhi, T.U. Bhatt, and A.P. Tiwari. A mathematical model for total power control loop of large PHWRs. *IEEE Transactions on Nuclear Science* 46: 1901-1911 (2016).
11. V.S. Volodin, and A.O. Tolokonskii. Parameters settings of NPP automatic regulators via analytical simulators. *XIII International Youth Scientific and Practical Conference* 317-326 (2017).
12. A.P. Tiwari, T.U. Bhatt, and P.V. Surjagade. Modelling and spatial control of 540 MWe pressurized heavy water reactor. *Transactions on Indian National Academy of Engineering* 06: 731-753 (2021).
13. S. Banerjee, D. Bose, A. Hazra, S. Chattopadhyay, and K. Ghosh. Controller design for operation of a 700 MWe PHWR with limited voiding. *Nuclear Engineering and Design* 357: 1-12 (2020).
14. M.C. Darling, G.F. Luger, T.B. Jonesy, M.R. Denman, and K.M. Groth. Intelligent modeling for nuclear power plant accident management. *International Journal on Artificial Intelligence Tools* 27: 1-25 (2018).
15. A.H. Malik, A.A. Memon, and F. Arshad. Fractional order modelling and robust multi-model intelligent controllers' synthesis for ACP1000 nuclear power plant. *Mehran University Research Journal of Engineering and Technology* 41: 43-53 (2022).
16. M.F. Shidik, and R.S.N. Mahmudah. Safety analysis of advanced CANDU reactor-700 (ACR-700) during transient and emergency condition using ACR simulator. *Journal of Sains Dasar* 10: 30-35 (2021).